Carbohydrate Polymers 87 (2012) 701–706

Contents lists available at SciVerse ScienceDirect

Carbohydrate Polymers

journal homepage: www.elsevier.com/locate/carbpol

Studies on the plasticization efficiency of deep eutectic solvent in suppressing the crystallinity of corn starch based polymer electrolytes

S. Ramesh [a,*], R. Shanti [b], Ezra Morris [b]

[a] Centre for Ionics University Malaya, Department of Physics, Faculty of Science, University of Malaya, 50603 Kuala Lumpur, Malaysia
[b] Faculty of Engineering and Science, Universiti Tunku Abdul Rahman, 53300 Kuala Lumpur, Malaysia

ARTICLE INFO

Article history:
Received 10 June 2011
Received in revised form 11 August 2011
Accepted 18 August 2011
Available online 25 August 2011

Keywords:
Corn starch
Deep eutectic solvent
Ionic conductivity
Transit site
Neutral ion multiple

ABSTRACT

A series of polymer electrolytes composed of corn starch (CS), lithium bis(trifluoromethanesulfonyl)imide (LITFSI) and deep eutectic solvent (DES) were fabricated by solution casting technique. The DES was synthesized from a mixture of choline chloride and urea at a molar ratio of 1:2. The addition of DES is crucial in enhancing the room temperature ionic conductivity by increasing the amorphous elastomeric phase in CS:LITFSI matrix. The ionic transport mechanism is improved and appreciable amount of ion conducting polymer electrolytes is produced. The highest ionic conductivity achieved for the polymer electrolyte composition CS:LiTFSI:DES (14 wt.%:6 wt.%:80 wt.%) is 1.04×10^{-3} S cm^{-1}. The anomalies that were observed with the addition of DES upon formation of neutral ion multiples were visually revealed by the SEM micrographs. The possible dipole–dipole interaction between the constituents was visualized by the FTIR spectroscopy upon change in cage peaks.

1. Introduction

In recent years, the negative impacts of inventions employing synthetic type of polymer electrolytes have come to light. Thus, scientists have been working on numerous approaches to replace the synthetic polymer electrolytes with some other promising alternatives. One such attempt to replace the conventional polymer electrolytes with completely biodegradable polymer electrolytes by utilizing a type of natural polymer namely corn starch (CS) is presented in this study.

The above mentioned natural polymer gains importance in the current development due to its biodegradable nature combined with several other promising properties such as low cost, independent of petroleum sources, availability of renewable resources and non-toxic nature (Vieira, Avellaneda, & Pawlicka, 2007; Wu, Wang, Li, Li, & Wang, 2009; Xu, Miladinov, & Hanna, 2004). Besides that, the ease in dissolving the CS in distilled water without the use of organic solvents can be considered as an additional advantage. Although there are numerous advantages of utilizing natural polymers, generally, this type of polymers are not practically used in the development of polymer electrolytes due to its high crystalline nature. The crystalline nature is induced by the presence of hydroxyl (–OH) functional groups where the attached hydrogen atom is small in size and fits well into the lattice and make it appear in a highly coordinated form. The strong hydrogen bonding in –OH functional group is another factor for the high crystallinity. These critical factors limit the maximum ionic conductivity that can be achieved by CS in the development of polymer electrolytes.

In this work, an attempt was made to resolve the stated barrier by incorporating selected additives. Initial efforts were done by incorporating with LiTFSI, a type of ionic salt, to resolve the mentioned limitations. This type of ionic salt is of special interest due to its large electronegativity and delocalization of charge (Ramesh & Lu, 2008). These properties contribute to the complete dissociation of LiTFSI in the polymer matrix and allow the two different charges of ions to remain in its ionic state as depicted below:

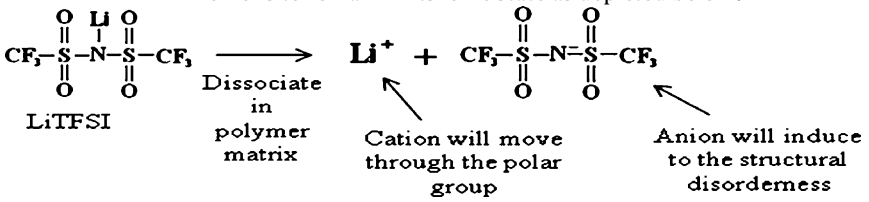

Only the anion ($TFSI^-$) will contribute to the structural disorderliness in the CS matrix whereas the cation (Li^+) will move along the polar functional group in CS. Since the selected anion is bigger

* Corresponding author. Tel.: +60 3 79674391.
E-mail address: rameshtsubra@gmail.com (S. Ramesh).

0144-8617/$ – see front matter © 2011 Elsevier Ltd. All rights reserved.
doi:10.1016/j.carbpol.2011.08.047

in size, it will not be able to move freely in between the segments to induce massive structural disorderliness. Hence, only a slight increase in the amorphous region will be induced which is not sufficient to exhibit an appreciable enhancement in the ionic conductivity.

To resolve the above-mentioned drawback, ionic mixture (DES) synthesized from the mixture of choline chloride and urea (Abbott, Capper, Davies, Rasheed, & Tambyrajah, 2003) was incorporated in order to attain high conducting polymer electrolytes. The dissolution of DES in the non-plasticized matrix will make the highly electronegative chloride ions (Cl^-) to detach from the molecular structure. Due to the small size of the Cl^- ions, they move freely in between the polymer segments. This incorporation is capable of increasing the structural disorderliness in CS:LiTFSI matrix allowing the DES-plasticized polymer electrolytes to be in a highly amorphous state. In addition, the highly electronegative Cl^- tends to detach more hydrogen atoms that have initially bonded with oxygen in –OH functional group in the polymer chain to make the oxygen unoccupied. This would allow more availability of transit site for lithium conducting ions (Li^+) to move within the polymer backbone extensively to increase the ionic transport mechanism for better ion conduction.

The benefit of employing DES in CS based polymer electrolytes is not limited to structural disorderliness but also has other outstanding properties such as sustainability, an unusual solvent property that further dissolves the highly crystalline CS, cheaper due to the low cost of raw materials, ease in the preparation method ignoring the purification process and requires no medium, non-toxic formulations and biodegradable (Hou et al., 2008; Jhong, Wong, Wan, Wang, & Wei, 2009; Zhang, Wu, Chen, Feng, & Bu, 2009).

In this study, we report the influence of different DES content in plasticizing CS:LiTFSI polymer electrolytes by using various characterization techniques to deduce the exerted room temperature ionic conductivity, structural morphology and complexation.

2. Experimental

2.1. Materials

Natural polymer, CS was purchased from Aldrich whereas the ionic salt, LiTFSI was procured from Fluka. The starting materials to synthesize DES which are choline chloride and urea were obtained from Sigma. All the starting materials were used as received. Distilled water was used as the solvent.

2.2. Preparation of polymer electrolytes

2.2.1. Synthesizing deep eutectic solvent (DES)

An appropriate amount of choline chloride and urea in the ratio of 1:2 were placed in a small clean beaker. These solid form chemicals were heated up under a stirring environment till the entire solids dissolve and appear as a colorless viscous solution.

2.2.2. Sample casting technique

The biodegradable polymer electrolytes were fabricated by dissolving an appropriate amount of CS as shown in Table 1 in 15 ml of distilled water, resulting in a milky solution. This solution was then gelatinized and a transparent solution was obtained upon heating at 75 °C under constant stirring. After the heating process, the solution was cooled down at ambient temperature under constant stirring for about 30 min. Then an appropriate amount of LiTFSI and the synthesized DES were added into the viscous solution and again the solution was allowed to stir for another hour to produce a homogeneous solution. The homogeneous solution was then cast on a clean Teflon plate and left to dry in the oven at 55 °C for 8 h.

Table 1
Composition ratio of CS:LiTFSI:DES polymer electrolytes with the respective designations.

Polymer electrolyte (CS:LiTFSI:DES) (wt.%)	Designation
70:30:0	DES-0
63:27:10	DES-10
56: 24:20	DES-20
49:21:30	DES-30
42:18:40	DES-40
35:15: 50	DES-50
28:12:60	DES-60
21:9:70	DES-70
14:6:80	DES-80
7:3:90	DES-90

2.3. Characterization

2.3.1. Impedance spectroscopy

The thickness of the thin films was measured with a micrometer screw gauge before the ionic conductivity testing was performed using a HIOKI Model 3532-50 Hi-Tester. All the measurements were taken over the frequency range extending from 50 Hz to 5 MHz with each thin film sandwiched between the two stainless steel blocking electrodes with an area of 4.9807 cm^2. The obtained impedance plot was used to find the bulk resistance (R_b) value which was then substituted in Eq. (1) to calculate the exerted ionic conductivity:

$$\sigma = \frac{L}{R_b A} \quad (1)$$

where σ is the ionic conductivity in S cm^{-1}, L is the thickness of the thin film sample in cm, R_b is the bulk resistance in Ω obtained from Cole–Cole impedance plot and A represents the surface area of the stainless-steel blocking electrodes in cm^2.

2.3.2. Scanning electron microscopy (SEM)

Selected samples were coated with a thin layer of gold before the SEM micrographs were captured using Leica's SEM (model S440) at 6 kV. The coating step is crucial to prevent electrostatic charging. All the micrographs were captured with the magnification factor of 500×.

2.3.3. Fourier transform infrared (FTIR)-horizontal attenuated total reflection (HATR) analysis

The occurrence of complexation between the chemical constituents was analyzed using Perkin-Elmer FTIR Spectrometer, Spectrum RX1, with the aid of a HATR compartment. The FTIR spectra were recorded in the transmittance mode in the wave region ranging from 4000 to 600 cm^{-1} with the resolution of 4 cm^{-1}.

3. Results and discussion

3.1. Conductivity studies at room temperature

Fig. 1 depicts the variation of ionic conductivity when the DES content in CS:LiTFSI:DES polymer electrolytes is increased from 0 wt.% to 90 wt.%. The ionic conductivity plot was sub divided into four regions to ease discussion on the exerted ionic conductivity trend.

From Fig. 1, it can be seen that the ionic conductivity of CS:LiTFSI polymer electrolytes improved with the initial incorporation of DES. Further increase in the DES content contributes an appreciable enhancement in this property as revealed by sample DES-20. This was ascribed to the increase in the number of lithium conducting ions (Li^+) that excessively migrates along the polymer backbone chain via forming coordination with the unoccupied oxygen atom. The unoccupied oxygen was obtained upon breaking of hydrogen bond in the hydroxyl (–OH) functional group in polymer backbone.

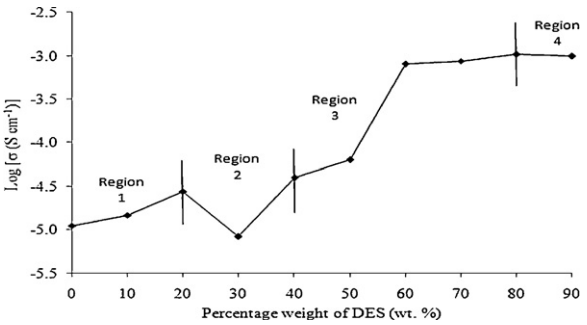

Fig. 1. Ionic conductivity (σ) of CS:LiTFSI:DES polymer electrolytes with different [Amim] Cl content at room temperature.

The disruption in the hydrogen bond suppresses the crystallinity in CS matrix, allowing more amorphous region (disordered form that results in more free volume) to be available to ease the mobility of Li^+ ions that are responsible in enhancing the ionic conductivity (Uma, Mahalingam, & Stimming, 2003).

Besides that, the presence of chloride free ions (Cl^-) obtained upon dissociation of DES in the CS matrix provides an alternative pathway for ions motion by allowing the Li^+ ions to temporarily form coordination on its transit sites while the neighboring oxygen atom being vacated (Yahya et al., 2006). This aids the hopping of Li^+ ions from one oxygen vacant site to another with ease and the increase in the capacity of ionic transfer enhances the ionic conductivity.

Further addition of DES above 20 wt.% (Region 2) induces an abrupt drop in the ionic conductivity. The reason for this slump was attributed to the possible conglomeration of excess DES particles forming neutral ion multiples (Ramesh & Lu, 2008). The ion aggregates will reduce the polymer–ionic mixture interface thereby blocking the existing conducting pathways (Anantha & Hariharan, 2005; Winie, Ramesh, & Arof, 2009). In accordance to this phenomenon, the extent of Li^+ ion transport will diminish due to the restriction on its mobility which subsequently decreases the ionic conductivity. As DES content is increased to 40 wt.%, the conducting pathways are again created by the dissociation of ion aggregates into free ions, imparting greater availability of amorphous region and additional transit site in forming coordination to facilitate the Li^+ ions mobility which aid in enhancing the ionic conductivity.

In Region 3, a considerable increase in the ionic conductivity was initially observed for sample DES-50 before a drastic increase accounted for the sample with 60 wt.% of DES. The increase in ionic conductivity shares a similar reason as in Region 1. The drastic increase in ionic conductivity provides an insight on the radical improvement in the structural disorderliness which induces a vast presence of amorphous fraction in the material which significantly improves the ion transport mechanism. Further increase in the DES content contributes to an almost constant increase in the ionic conductivity. The maximum room temperature ionic conductivity of 1.04×10^{-3} S cm^{-1} is achieved by sample DES-80. Further incorporation of DES content accounts to a slight decrease in this property as observed in Region 4. The observed decline in ionic conductivity was attributed to the formation of neutral ion multiples that causes a decrease in the mobility of Li^+ ions which are crucial in improving the ionic conductivity.

3.2. SEM studies

The exerted ionic conductivity trend in Region 2 can be further validated by relying on the SEM photographs that describes the surface morphology of the samples. The surface morphology of the polymer electrolytes has been presented in Fig. 2(a)–(c).

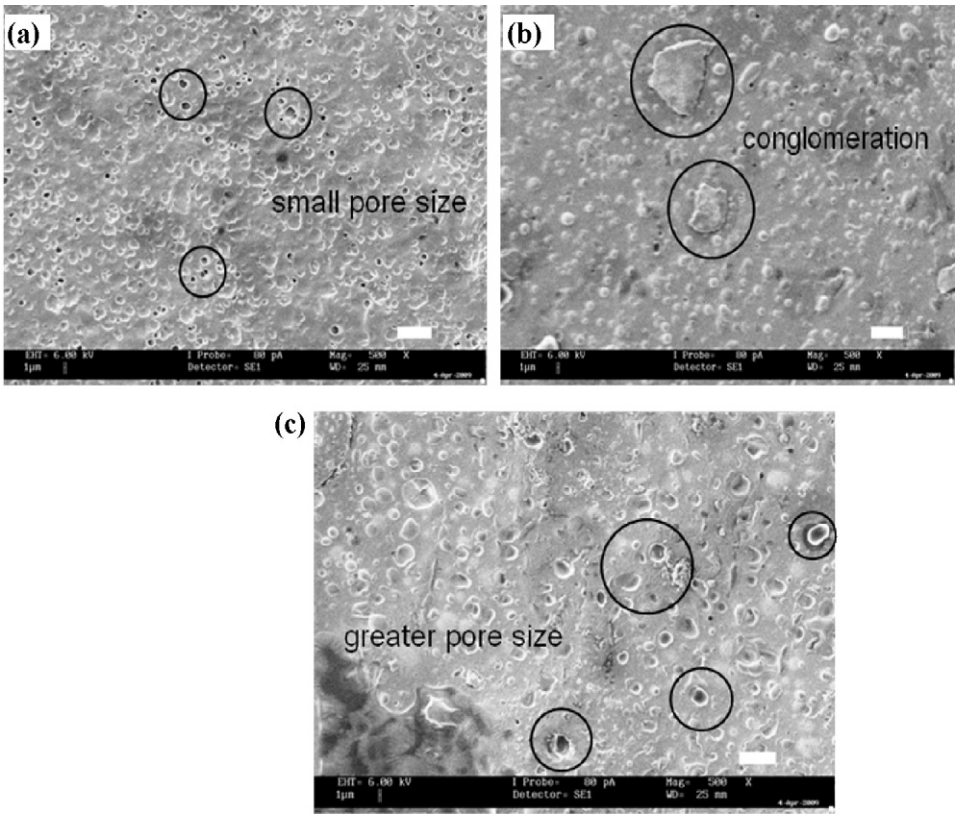

Fig. 2. SEM micrographs of CS:LiTFSI:DES matrix when different content of DES being incorporated in such (a) DES-20, (b) DES-30 and (c) DES-40.

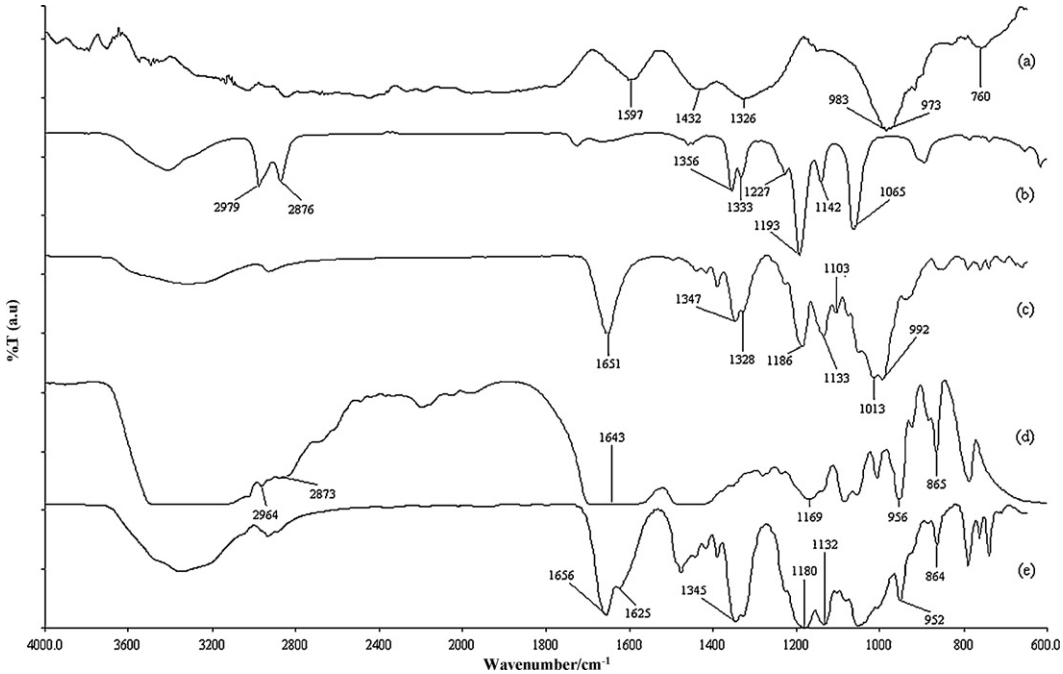

Fig. 3. FTIR spectra for (a) pure CS, (b) pure LiTFSI, (c) DES-0, (d) pure DES and (e) DES-80.

Based on the SEM image in Fig. 2(a), it can be noted that the sample DES-20 is highly packed with small spheres having an average diameter of 5.4 μm, with some spheres embedded with small pores. These spheres represent the crystalline region where it consists of a number of platelets or lamellae radiating from a nucleating centre, called spherulites (Paradhan, Choundhary, & Samantaray, 2008; Singh, Kim, & Rhee, 2008). The regions between the neighboring lamellae show the existence of amorphous phase involved in ion conduction. This observation reveals the high order of atoms which makes it appear in a semi-crystalline nature.

Further addition of 30 wt.% of DES gradually modifies the porous microstructure to less porous membranes. This was attributed to the conglomeration of excess DES particles forming neutral ion aggregates (as circled in Fig. 2(b)) near the pores that consequently reduces the pore size and porosity (Deka & Kumar, 2009). This in turn, decreases the uptake of liquid electrolyte in the microporous membrane resulting in lower ionic conductivity.

Other plausible reason in explaining the drop in the ionic conductivity of sample DES-30 can be inferred from the placement of ion aggregates covering the amorphous phase which blocks the existing conducting pathways. Since ion migration is only allowed in amorphous regions thus the corresponding blockage restricts the ions mobility and causes an abrupt reduction in the ionic conductivity.

In Fig. 2(c), the disappearance of ion aggregates on the surface morphology upon addition of 40 wt.% DES reveals the dissociation of neutral ion multiples into charge carriers. Hence, conducting pathways are again created for the Li^+ ion transport which would subsequently enhance the ionic conductivity. The neutral charge borne by the ion aggregates will make it to be present in an unstable condition that easily disrupts upon addition of small amount of free ions (from DES).

Other observation to suggest the improvement in ionic conductivity was the increase in both the number of voids and pore size with an average diameter of 9.6 μm (Fig. 2(c)). The increase in the number of void correlates to the significant disruption in the crystalline region that enhances the amorphous fraction present between the spheres. Since the ion transport only occurs predominantly in amorphous phase thus an increase in ionic conductivity will be observed for sample DES-40. In addition, the increase in the pore size reveals the increase in the porosity of the membrane which entraps large volumes of the liquid electrolyte in the cavities (Saikia, Chen-Yang, Chen, Li, & Lin, 2008, 2009) accounting to the ease in the Li^+ ions mobility which then enhances the ionic conductivity.

3.3. FTIR-HATR studies

This analysis is a promising method to deduce the complexation between the chemical constituents present in both crystalline and amorphous phase. This was deduced by relying on the changes in cage peak in terms of the wavenumber shifting, relative intensity, shape, peak disappearance and also through the formation of new peaks. All the observable changes in cage peak attributed to the complexation have been reported.

The band assignments for respective pure substances were summarized in Table 2 (Ning, Xingxiang, Haihui, & Benqiao, 2009; Ramesh & Lu, 2008). FTIR spectra of pure CS, pure LiTFSI, DES-0, pure DES and DES-80 were presented in Fig. 3. The complexation between pure CS and LiTFSI can be deduced based on the FTIR spectrum of DES-0 represented in Fig. 3(c). The first evidence to prove the complexation was based on new peaks formation at 1651 cm^{-1}

Table 2
Band assignments and wavenumbers exhibited by pure constituents namely CS, LiTFSI and DES.

Sample	Band assignments	Wavenumber (cm^{-1})
CS	δ (O–H) bending of H_2O	1597
	CH_2 symmetric bending	1432
	CH_2 wagging	1326
	C–O–C	760–983
	S–CH_3	2979 and 2876
LiTFSI	C–SO_2–N	1356
	–CF_3	1193
	C–F stretch	1142
	S=O	1065
DES	C–H stretching (CH_3)	2964
	C–H stretching (CH_2)	2873
	C=O	1643
	Ammonium ion	1169

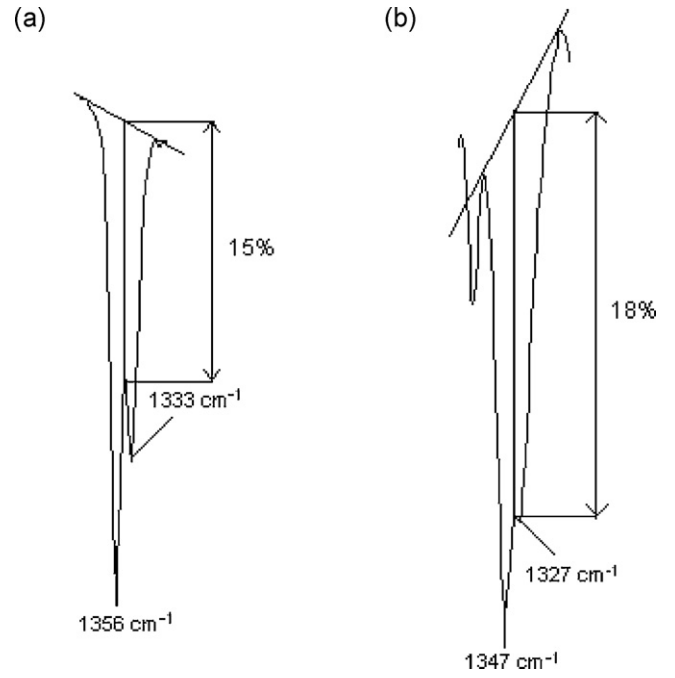

Fig. 4. The change in intensity of C–SO_2–N band for (a) pure LiTFSI and (b) DES-0.

and 1103 cm^{-1} in DES-0. This implies that some degree of complexation has occurred and new phase has formed between the LiTFSI and the oxygen atom of the hydroxyl (–OH) group in CS.

Additionally, the peaks at 1356 cm^{-1} and 1333 cm^{-1} that corresponds to C–SO_2–N bonding in pure LiTFSI was shifted to lower wavenumber at 1347 cm^{-1} and 1328 cm^{-1} upon mixing with CS. This shows the coordination of free hydrogen atom with nitrogen at these wavenumbers. Besides that, the relative intensity of this peak increases from 15% (pure LiTFSI) to 18% after complexation with pure CS as depicted in Fig. 4.

The characteristic peaks of CF_3 and C–F stretch that co-exist at 1193 and 1142 cm^{-1}, respectively in pure LiTFSI was shifted to lower wavenumber at 1186 and 1133 cm^{-1} in DES-0 upon complexation with pure CS. Further evidence to prove the complexation was based on the peaks that fall in the range of 1100–1300 cm^{-1} in pure LiTFSI which splits from 3 to 4 individual peaks and allocated at lower wavenumber in DES-0 upon complexation with pure CS. The final observable change proves the miscibility of LiTFSI in CS matrix was the two peaks at 983 and 973 cm^{-1} in pure CS which was reallocated to higher wavenumber at 1013 and 992 cm^{-1}, respectively in DES-0. This wavenumber shifting illustrates the weaker interaction between Li^+ ions and oxygen atom in C–O–C group.

The incorporation of DES in CS:LiTFSI matrix was believed to involve in complexation and this was evident based on the changes in cage peak that has been presented in Fig. 3(e). The peak at 1651 cm^{-1} in DES-0 underwent change in shape from one to two peaks and is consequently reallocated at higher wavenumber (1656 cm^{-1}) upon complexation with pure DES. Besides that, this particular peak also undergoes band broadening being effect of DES addition. Another evidence of complexation was the peak at 1347 cm^{-1} (DES-0) which shifted to lower wavenumber at 1345 cm^{-1} (DES-80) upon addition of DES. This shifting proves the substitution of initially bonded lithium to the nitrogen with hydrogen atom. The reference peak also underwent increase in relative intensity from 22% (DES-0) to 66% (DES-80) upon complexation.

The displacement of peak initially present at 1186 cm^{-1} in non-plasticized sample to 1180 cm^{-1} in DES plasticized sample also reveals possible interaction. The peak at 1133 cm^{-1} in DES-0 shifted to lower wavenumber at 1132 cm^{-1} upon addition of 80 wt.% of DES. The peaks present at 956 and 865 cm^{-1} in pure DES was shifted to lower wavenumber at 952 and 864 cm^{-1}, respectively in DES-80.

The observed changes in the cage peaks indicate that some degree of co-ordination or complexation had occurred between the constituents. The similarity between the FTIR spectra for each sample indicates that LiTFSI and DES are physically bonded with CS.

4. Conclusion

A series of biodegradable polymer electrolytes were developed by plasticizing the CS:LiTFSI matrix with DES up to a maximum addition of 90 wt.%. The highest ionic conductivity was obtained for sample containing 80 wt.% of DES with the calculated ionic conductivity value of 1.04×10^{-3} S cm^{-1} at room temperature. This sample composition appears as the highest conducting polymer electrolyte due to the presence of greater amorphous elastomeric phase that improves the ionic transport mechanism. SEM micrographs were used to review the possible formation of neutral ion multiples which induce a certain decrease in the ionic conductivity. The occurrence of some degree of co-ordination between the chemical constituents was revealed by the FTIR spectra.

Acknowledgement

This work was supported by the Universiti Malaya Research Grant (UMRG: RG140-11AFR).

References

Abbott, A. P., Capper, G., Davies, D. L., Rasheed, R. K., & Tambyrajah, V. (2003). Novel solvent properties of choline chloride/urea mixture. *Chemical Communications*, *39*, 70–71.

Anantha, P. S., & Hariharan, K. (2005). Physical and ionic transport studies on poly(ethylene oxide)–$NaNO_3$ polymer electrolyte system. *Solid State Ionics*, *176*, 155–162.

Deka, M., & Kumar, A. (2009). Ionic transport in P(VdF-HFP)-PEO based novel microporous polymer electrolytes. *Bulletin of Material Science*, *32*, 627–632.

Hou, Y., Gu, Y., Zhang, S., Yang, F., Ding, H., & Shan, Y. (2008). Novel binary eutectic mixtures based on imidazole. *Journal of Molecular Liquids*, *143*, 154–159.

Jhong, H. R., Wong, D. S., Wan, H. C., Wang, C. Y., & Wei, Y. T. C. (2009). A novel deep eutectic solvent-based ionic liquid used as electrolyte for dye-sensitized solar cells. *Electrochemistry Communications*, *11*, 209–211.

Ning, W., Xingxiang, Z., Haihui, L., & Benqiao, H. (2009). 1-Allyl-3-methylimidazolium chloride plasticized-corn starch as solid biopolymer electrolytes. *Carbohydrate Polymer*, *76*, 482–484.

Paradhan, D. K., Choundhary, R. N. P., & Samantaray, B. K. (2008). Studies of dielectric relaxation and AC conductivity behaviour of plasticized polymer nanocomposite electrolytes. *International Journal of Electrochemical Science*, *3*, 597–608.

Ramesh, S., & Lu, S. C. (2008). The effect of nanosized silica in poly(methyl methacrylate)-lithium bis(trifluoromethanesulfonyl)imide based polymer electrolytes. *Journal of Power Sources*, *185*, 1439–1443.

Saikia, D., Chen-Yang, Y. W., Chen, Y. T., Li, Y. K., & Lin, S. I. (2008). Investigation of ionic conductivity of composite gel polymer electrolyte membranes based on P(VDF-HFP), $LiClO_4$ and silica aerogel for lithium ion battery. *Desalination*, *234*, 24–32.

Saikia, D., Chen-Yang, Y. W., Chen, Y. T., Li, Y. K., & Lin, S. I. (2009). ^{7}Li NMR spectroscopy and ion conduction mechanism of composite gel polymer electrolyte: A comparative study with variation of salt and plasticizer with filler. *Electrochimica Acta*, *54*, 1218–1227.

Singh, P. K., Kim, K. W., & Rhee, H. W. (2008). Electrical, optical and photoelectrochemical studies on a solid PEO-polymer electrolyte doped with low viscosity ionic liquid. *Electrochemistry Communications*, *10*, 1769–1772.

Uma, T., Mahalingam, T., & Stimming, U. (2003). Mixed phase solid polymer electrolytes based on poly(methylmethacrylate) systems. *Materials Chemistry and Physics*, *82*, 478–483.

Vieira, D. F., Avellaneda, C. O., & Pawlicka, A. (2007). Conductivity study of a gelatin-based polymer electrolyte. *Electrochimica Acta*, *53*, 1404–1408.

Winie, T., Ramesh, S., & Arof, A. K. (2009). Studies on the structure and transport properties of hexanoyl chitosan-based polymer electrolytes. *Physica B: Condensed Matter*, *404*, 4308–4311.

Wu, R. L., Wang, X. L., Li, F., Li, H. Z., & Wang, Y. Z. (2009). Green composite films prepared from cellulose, starch and lignin in room-temperature ionic liquid. *Bioresource Technology*, *100*, 2569–2574.

Xu, Y., Miladinov, V., & Hanna, M. A. (2004). Synthesis and characterization of starch acetates with high degree of substitution. *Cereal Chemistry*, *81*, 735–740.

Yahya, M. Z. A., Ali, A. M. M., Mohammat, M. F., Hanafiah, M. A. K. M., Mustaffa, M., Ibrahim, S. C., et al. (2006). Ionic conduction model in salted chitosan membranes plasticized with fatty acid. *Journal of Applied Sciences*, *6*, 1287–1291.

Zhang, J., Wu, T., Chen, S., Feng, P., & Bu, X. (2009). Versatile structure-directing roles of deep eutectic solvents and their implication in generation of porosity and open metal sites for gas storage. *Angewandte Chemie International Edition English*, *48*, 3486–3490.